Novel Findings in Obstetric Brachial Plexus Palsy: A Study of Corpus Callosum Volumetry and Resting-State Functional Magnetic Resonance Imaging of Sensorimotor Network

Kishore Kislay, MCh*
Bhagavatula Indira Devi, MS, MCh*
Dhananjaya Ishwar Bhat, MCh*
Dhaval Prem Shukla, MCh*
Arun Kumar Gupta, MD‡
Rajanikant Panda, BE‡

*Departments of Neurosurgery, National Institute of Mental Health and Neurosciences (NIMHANS), Bangalore, India; ‡Departments of Neuroimaging and Interventional Radiology, National Institute of Mental Health and Neurosciences (NIMHANS), Bangalore, India

The results of this study were presented (platform presentation) in the "resident awards session" at the national annual conference of Indian Society for Pediatric Neurosurgery held at Mumbai, India from March 24-26 , 2017. This presentation was adjudged the best paper. The abstract/paper has not been published.

Correspondence:
Bhagavatula Indira Devi, MS, MCh,
Department of Neurosurgery,
Second floor, Neurosciences Faculty Block,
National Institute of Mental Health and Neurosciences (NIMHANS),
Hosur Road,
Bangalore 560029,
Karnataka, India.
E-mail: bidevidr@gmail.com

Received, April 25, 2017.
Accepted, September 11, 2017.
Published Online, October 28, 2017.

BACKGROUND: The response of the brain to obstetric brachial plexus palsy (OBPP) is not clearly understood. We propose that even a peripheral insult at the developmental stage may result in changes in the volume of white matter of the brain, which we studied using corpus callosum volumetry and resting-state functional magnetic resonance imaging (rsfMRI) of sensorimotor network.

OBJECTIVE: To study the central neural effects in OBPP.

METHODS: We performed an MRI study on a cohort of 14 children who had OBPP and 14 healthy controls. The mean age of the test subjects was 10.07 ± 1.22 yr (95% confidence interval). Corpus callosum volumetry was compared with that of age-matched healthy subjects. Hofer and Frahm segmentation was used. Resting-state fMRI data were analyzed using the FSL software (FMRIB Software Library v5.0, Oxford, United Kingdom), and group analysis of the sensorimotor network was performed.

RESULTS: Statistical analysis of corpus callosum volume revealed significant differences between the OBPP cohort and healthy controls, especially in the motor association areas. Independent t-test revealed statistically significant volume loss in segments I (prefrontal), II (premotor), and IV (primary sensory area). rsfMRI of sensorimotor network showed decreased activation in the test hemisphere (the side contralateral to the injured brachial plexus) and also decreased activation in the ipsilateral hemisphere, when compared with healthy controls.

CONCLUSION: OBPP occurs in an immature brain and causes central cortical changes. There is secondary corpus callosum atrophy which may be due to retrograde transneuronal degeneration. This in turn may result in disruption of interhemispheric coactivation and consequent reduction in activation of sensorimotor network even in the ipsilateral hemisphere.

KEY WORDS: Obstetric brachial plexus palsy, Resting-state fMRI, Cortical plasticity, Corpus callosum volume

Neurosurgery 83:905–914, 2018 DOI:10.1093/neuros/nyx495 www.neurosurgery-online.com

The human brain continues to develop well beyond the fetal period as the process of myelination and maturation occurs.[1-3] Maturation involves formation of new synapses. Obstetric brachial plexus palsy (OBBP) occurs at the time of childbirth, when none of these are complete. The brain's response to OBBP is not well established.

Brachial plexus injury (BPI) results in insult to the descending motor projections and sensory input. Alterations in the circuitry of brain may be expected to occur in OBPP, which occurs at an immature stage of brain development.

ABBREVIATIONS: BPI, brachial plexus injury; **DTI,** diffusion tensor imaging; **EPI,** echo-planar images; **FSL,** FMRIB Software Library; **GLM,** general linear model; **IC,** independent component; **ICA,** independent component analysis; **MELODIC,** multivariate exploratory linear decomposition into independent components; **OBPP,** obstetric brachial plexus palsy; **PICA,** probabilistic independent component analysis; **rsfMRI,** resting-state functional magnetic resonance imaging; **TFCE,** threshold-free cluster enhancement

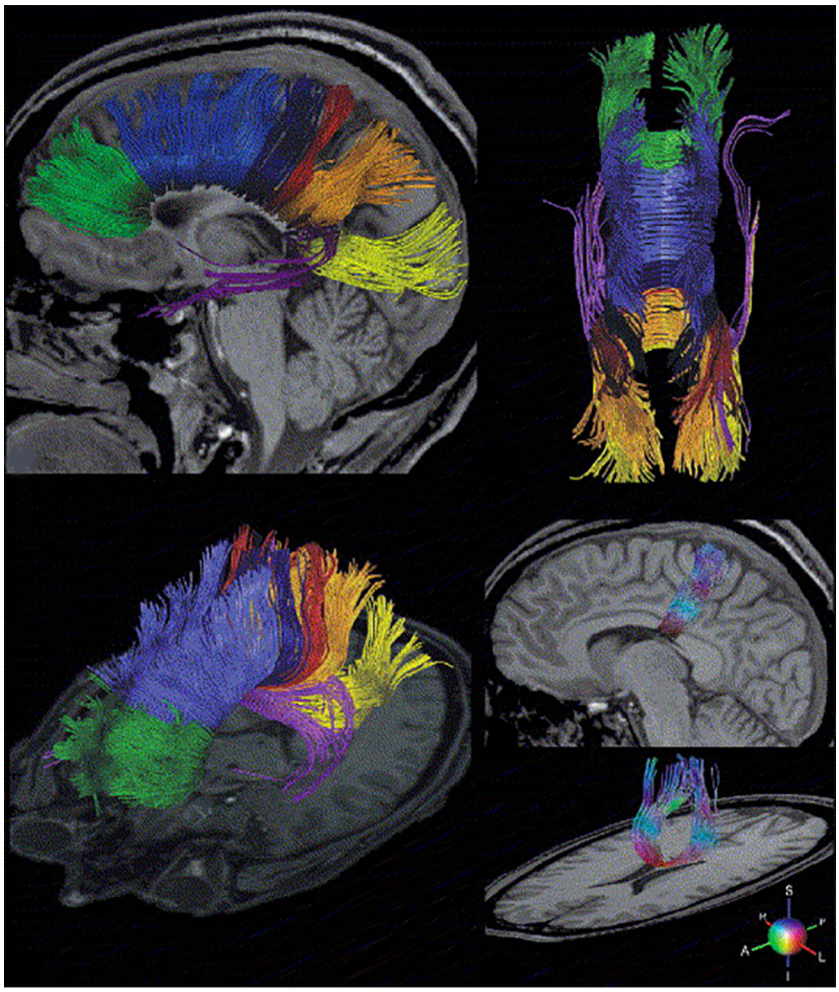

FIGURE 1. *Transcallosal fiber tracts from a single male subject overlaid onto individual anatomical reference images. Sagittal, top, and oblique views of a 3-dimensional reconstruction of all callosal fibers comprising bundles projecting into the prefrontal lobe (coded in green), premotor and supplementary motor areas (light blue), primary motor cortex (dark blue), primary sensory cortex (red), parietal lobe (orange), occipital lobe (yellow), and temporal lobe (violet). Sagittal and oblique views of callosal fiber tracts that project into the primary motor cortex. The colors correspond to the local mean diffusion direction as indicated by the color code in the lower right of the figure: A, anterior; I, inferior; L, left; P, posterior; R, right; S, superior. Reprinted from Hofer and Frahm,[23] with permission from Elsevier.*

Following peripheral nerve injury, there is anterograde (Wallerian) and retrograde axonal degeneration. Due to loss of afferent and efferent signals and disruption of cortical input, cortical inactivity and degeneration is only to be expected.[4-6] This in turn may result in changes in white matter volume and interhemispheric connectivity.[7-10] White matter volume changes would be reflected in corpus callosum volumetry.[11-15] As a corollary, disruption of interhemispheric coactivation may result in bilateral effects on the brain.

Resting-state functional magnetic resonance imaging (rsfMRI) of the brain is a technique wherein multiple functional networks can be studied in a brain.[16-18] This is especially helpful in subjects who are unable to perform the required task. Multiple studies have been performed in adults with traumatic BPI using rsfMRI, and cortical plasticity has been demonstrated.[19-22] It is a good tool to study the pattern of interhemispheric coactivation.

The corpus callosum is the main white matter bundle which connects both the hemispheres and is the major substrate for interhemispheric coactivation. Interthalamic adhesion and anterior commissure may have minor contributions.[7,9,10] Diffusion tensor imaging and fiber tractography have shown that different segments of corpus callosum carry fibers from

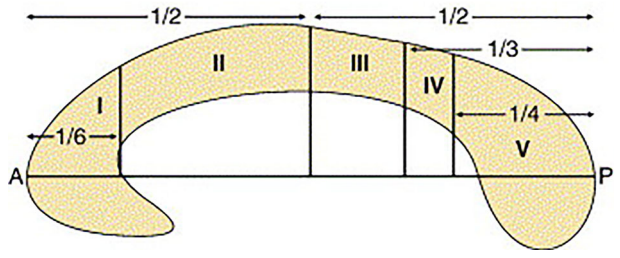

FIGURE 2. *Topography of the midsagittal corpus callosum. Hofer and Frahm's classification.[23] Region I: prefrontal; region II: premotor and supplementary motor; region III: motor; region IV: sensory; region V: parietal, temporal, and occipital. A, anterior; P, posterior. Reprinted from Hofer and Frahm,[23] with permission from Elsevier.*

different regions of the cerebrum[23] (see Figures 1 and 2). Hofer and Frahm[23] parcellated the corpus callosum into 5 segments based on the cerebral regions:

- Segment I—anterior sixth; prefrontal area
- Segment II—beyond anterior sixth up to anterior half; premotor and supplementary motor area
- Segment III—first sixth beyond anterior half; primary motor area
- Segment IV—first twelfth beyond segment III; primary sensory area
- Segment V—posterior quarter; parietal-temporal-occipital area

Objectives

This study was aimed to examine the central neural effects of OBPP, which is a peripheral nerve injury, in a developing brain.

METHODS

Study Design

This was an observational cross-sectional study conducted over 3 years (2013-2016). Patients were recruited from neurosurgery outpatient department of our hospital.

OBPP Group

The inclusion criterion was occurrence of OBPP, irrespective of previous intervention. Following institute ethics committee clearance, 14 patients were included in the study. The mean age of the subjects was 10.07 ± 1.22 yr (95% confidence interval). Children with history of perinatal asphyxia (determined by either documentation in obstetrical records or MRI features suggestive of encephalomalacia/leukomalacia or deep nuclei changes) or hydrocephalus, which could confound volumetric analysis, were excluded from the study.

Healthy Controls

Fourteen age-matched healthy controls were taken from our pre-existing database. Mean age was 12.92 ± 1.50 yr (95% confidence interval).

Ethical Clearance

The consent for participating in the study was obtained from the child's parents and also the child. They were explained that regardless of the inclusion, standard care would be continued. A clinical proforma was generated and all the demographic details were collected.

MRI Data Acquisition

Resting-state fMRI was acquired using a 3T scanner (Skyra, Siemens, Erlangen, Germany). We use these MRI parameters for all the rsfMRI-based studies in our Institute. One hundred eighty-five volumes of gradient-echo, echo-planar images (EPI) were obtained using the following parameters: 36 slices, 4 mm slice thickness in interleaved manner with a field of view of 192 × 192 mm, echo time 35 ms, repetition time 3000 ms, re-focusing pulse 90°, voxel size-3 × 3 × 4 mm, and matrix- 256 × 256 × 114. A T1-weighted 3-dimensional magnetization prepared rapid acquisition gradient echo (T1 3D MPRAGE) sequence was acquired for anatomical information (with the voxel size 1 × 1 × 1 mm, 192 × 192 × 256 matrix).

Corpus Callosum Volumetry

Corpus callosum volumetry was done using a rule-based automated segmentation technique with the help of C8 software,[24] which is based on SPM platform.

Workflow[25]

1. Data preparation
2. Preprocessing
   a. Midsagittal plane extraction
   b. Automated corpus callosum segmentation with optional manual editing
   c. Thickness profile generation and areal parcellation
   d. Project segmentation and parcellations to native space
3. Statistical testing of group-wise thickness profile.

We used Hofer and Frahm[23] parcellation technique for segmental volumetry.

Resting-State fMRI Preprocessing

Analysis of rsfMRI images was done using FSL (FMRIB Software Library v5.0, Oxford, United Kingdom).[26] Independent component analysis (ICA) was performed, and sensorimotor network was identified. The main tools used were fMRI Expert Analysis Tool and multivariate exploratory linear decomposition into independent components (MELODIC) modules. Signal equilibration was done after discarding first 5 functional images (EPI volumes) and 180 volumes were used for analysis. MCFLIRT[27] was used for motion correction, and Brain Extraction Toolbox[28] was used to remove nonbrain tissue (cerebrospinal fluid, scalp, etc). There were no significant head motion-related artifacts between the groups. Spatial smoothing was done using techniques described in the literature.[26,29,30] EPI volumes of each individual subject's high-resolution anatomical volumes were co-registered into MNI152 standard space template, and re-sampling was performed keeping the resolution at 3 mm using FNIRT (FMRIB nonlinear image registration tool).[31]

Independent Components

The technique of ICA was used to ascertain the functional connectivity. This data-driven approach allows us to extract voxel-wise

TABLE 1. Three-Dimensional Spatial Coordinates for Pre- and Postcentral Gyrus (Labeled by Automated Anatomical Labeling on SPM8, University College of London, United Kingdom), and Number of Voxels and t-Value (Intensity of Activation), *P*-Value < .05

	Brain region	X co-or	Y co-or	Z co-or	K (no. of voxels)	T-value
Patient_Right (internal control)	Postcentral_R	42	–26	60	950	8.1
	Precentral_R	32	–14	59	451	6.2
Patient_Left (test)	Postcentral_L	–48	–23	55	494	7.3
	Precentral_L	–30	18	60	221	6
Healthy Control_Right	Postcentral_R	36	–34	57	1375	11.9
	Precentral_R	38	–13	60	1031	9.2
Healthy Control_Left	Postcentral_L	–35	–34	52	1606	12.3
	Precentral_L	–25	–26	67	1476	9.4

functional networks based on their temporal and spatial fluctuations. FSL's MELODIC tool[29,30,32] was used to perform the probabilistic independent component analysis (PICA) and its data exploration was used to perform single-subject ICA. All extracted independent components (ICs) were visually inspected. Eye motion-related artifacts, high-frequency noise, field inhomogeneity, gradient instability, slice dropout, and breathing and heart rate-related artifacts were de-noised based on the existing literature using the command "fsl_regfilt" defined in FSL MELODIC.[26,29,30] The same tool was also used to perform multivariate group PICA and derive spatially ICs across all datasets (14 test subjects and 14 controls) which were temporally concatenated. Fast ICA algorithm was used to optimize the non-Gaussian spatial source distributions of 70 sets of independent vectors across temporal and spatial domains.

Dual Regression Analysis

Subject-specific time series and associated spatial maps were generated from the spatial maps obtained from group ICs.[32,33] The data components representing the sensorimotor area were identified from the set of group IC maps by visually comparing their anatomical location. The left and right hemisphere sensorimotor ICs are selected from the group ICs. To compare the injured hemisphere with healthy hemisphere of the control group, group-wise comparison was performed using dual regression. Statistical differences were assessed using threshold-free cluster enhancement (TFCE) technique.[34] Dual regression was carried out on the group IC data implemented in FSL, which allows voxel-wise comparisons of resting-state functional connectivity. It is a regression technique that performs reverse engineering of individual subject level data from each group-level component map (https://fsl.fmrib.ox.ac.uk/fsl/fslwiki/DualRegression).[26] The set of spatial maps derived from group-mean analysis was used to generate individual subject-specific spatial maps and temporal dynamics. This approach proceeds in 2 steps: the first involves the use of a full set of group IC spatial maps in a linear spatial regression model against separate fMRI datasets, providing the matrices describing subject-specific and component-specific temporal dynamics. Next, these time-course matrices for each subject are used to perform linear temporal regression against the associated rsfMRI dataset to generate subject-specific spatial maps. Finally, different component maps are collated across the subjects into a single 4D file. At this stage, the ICs of interest are identified for further analysis. In this study, left and right hemispheric sensorimotor networks were the IC components of interest, which were visually identified. Group differences for each spatial map were assessed using a voxel-wise general linear model (GLM)-based analysis. Nonparametric permutation (5000 permutations)-based testing with cluster-based thresholding using TFCE with cluster significance threshold of $P < .05$ was used to obtain suprathreshold cluster map. This resulted in spatial maps characterizing the test and control group differences. The GLM comparison included (1) injured hemisphere with healthy hemisphere of patient group and (2) patient and control group. Each of the components of interest was tested for difference between groups and group averages. To estimate group mean effects, the results were thresholded with family-wise error corrected at $P \leq .05$, applied for voxel-wise data. Then we used a false discovery rate correction ($P < .05$) for multiple comparisons on top of TFCE suprathreshold maps of each group. However, we did not find statistical significance due to limited number of samples. Therefore, the group differences were quantified by the cluster values and the intensity t-value of ICs spatial maps which were extracted after TFCE threshold for each group and condition (see Table 1).

Using the paradigm of experimental vs control, in a right BPI, the left hemisphere was presumed to be the "test" side and the right would be "internal control." Subgroup analysis was performed among the 3 groups: test, internal control, and healthy control.

The results in test subjects with corresponding hemispheres of healthy controls were also compared. During the study, we were curious to see what differences were in those who underwent intervention and those who did not. However, as the ICA of rsfMRI was performed for the entire group as a whole, we could not derive any meaningful results due to the small numbers. It was not technically feasible to subdivide patients into operated and nonoperated. The final output of sensorimotor network activation in rsfMRI is a mean of a group of patients. Usually, for meaningful results (ie, summated averaging of output for all patients), numbers in excess of 10 subjects are required. In this study, the small numbers did not permit us to further subanalyze the operated and nonoperated subjects.

Since the test group was heterogenous in terms of right and left side of obstetric BPI, the images were appropriately flipped to orient all the test hemispheres on left side. All the healthy controls were right-handed individuals.

Statistical Analysis

Statistical analysis was done using SPSS (IBM Corp. Released 2011. IBM SPSS Statistics for Windows, Version 20.0. Armonk, New York).

Two-tailed t-test was performed to detect significance ($P < .05$) between the segmental volumetry between the 2 groups.

TABLE 2. Clinical Profile of Patients with OBPP Who Underwent Neurotization

Subject	Age (in years) at presentation	Side	Diagnosis	Power at first visit (MRC grading 0-5)			Horner's	Intervention	Outcome at 1-yr follow up (MRC grading 0-5)	Narakas' grade (at birth)
				Sh.abd	Elb.flex	Distal				
KT	11	Right	Erb's	3	3	5	No	Pectoralis release elsewhere at age 3 yr, followed by axillary-IC neurotization at age 11 yr	Improved to 4/5	I
AG	9	Left	Erb's	3	3	5	No	IC-MC neurotization at age 9 yr	Improved to 4/5	I
NP	8	Right	Erb's	3	3	5	No	IC-MC neurotization at age 8 yr	Improved to 4/5	I
PK	12	Left	Pan-plexus	0	0	1	yes	IC-MC neurotization at age 5 yr	Not improved	IV

IC = intercostal nerve; MC = musculocutaneous nerve; MRC = Medical Research Council; Sh.abd = shoulder abduction; elb.flex = elbow flexion.

TABLE 3. Clinical Profile of Patients With OBPP Who Did Not Undergo Surgical Intervention

Subject	Age (in years) at presentation	Side	Diagnosis	Power at first visit (MRC grading 0-5)			Horner's	Intervention	Outcome at 1-yr follow up (MRC grading 0-5)	Narakas' grade (at birth)
				Sh.abd	Elb.flex	Distal				
TJ	12	Left	Erb's	4	4	5	No	Advised neurotization. Parents refused	??	I
SK	8	Left	Erb's	4	4	5	No	Physiotherapy	Unchanged	I
DK	5	Right	Pan-plexus	3	3	3	No	Physiotherapy	Unchanged	III
VL	10	Right	Pan-plexus	3	3	0	yes	Physiotherapy	Unchanged	IV
GK	13	Right	Pan-plexus	3	3	0	yes	Physiotherapy	Unchanged	IV
YO	11	Right	Pan-plexus	3	3	0	Yes	Physiotherapy	Unchanged	IV
SJ	9	Right	Pan-plexus	1	1	1	yes	Physiotherapy	Unchanged	IV
HK	10	Right	Pan-plexus	1	1	1	No	Physiotherapy	Unchanged	III
HF	14	Right	Pan-plexus	0	0	1	yes	Physiotherapy	Unchanged	IV
SG	9	Right	Pan-plexus	0	0	1	Yes	Physiotherapy	Unchanged	IV

IC = intercostal nerve; MC = musculocutaneous nerve; MRC = Medical Research Council; Sh.abd = shoulder abduction; elb.flex = elbow flexion.

For analysis of the results of rsfMRI, visual inspection of the images provided a subjective idea of the differential activation of the 2 sides. Further statistical quantification was made using dual regression analysis comparing the cluster values and t-values of the intensity of activation.

RESULTS

OBPP Group

The mean age in the current study was 10.07 ± 1.22 yr (95% confidence interval). Full-scale Medical Research Council grading and Narakas' grading[36] were used for clinical classification. Five of them had Erb's palsy and rest of them had pan-plexus palsy. All patients had zero active range of motion in shoulder and elbow at birth, and had been on regular physiotherapy. Immediate preoperatively (n = 4), power was 3/5 in 3 cases and 0/5 in 1 patient. Most of them (9/14) did obtain partial improvement in motor strength by the time they were referred to us. Postneurotization (n = 4) improvement was observed in 3 out of 4 patients. The only surgical intervention done prior to consultation with us was pectoralis release in one patient. Patients with Narakas' grade III and IV at birth did not recover well. Recovery was universally poor in the distal muscles (see Tables 2 and 3).

TABLE 4. Segmental Corpus Callosum Volume in Subjects With OBPP (Test) and Healthy Controls

Subject		Segment I		Segment II		Segment III		Segment IV		Segment V		Total volume	
Test	Control	Test	Control	Test	Control	Test	Control	Test	Control	Test	Control	Test	Control
KT	HC1	52.6875	60.0625	98.125	93.25	33.3125	32.8125	19.25	9.9375	109	57.25	312.375	253.3125
AG	HC2	67	98.3125	119	159.625	46.1875	61.25	15.0625	32.875	89.125	142.375	336.375	494.4375
NP	HC3	68.9375	69.6875	134.5625	105.6875	44.1875	39.75	14.125	17.3125	127.875	93.5625	389.6875	326
PK	HC4	69.3125	79.5625	121.3125	120.0625	54.875	30.3125	28.25	14.8125	155.25	118.1875	429	362.9375
TJ	HC5	51.625	56.6875	116.625	100.375	51.125	52	20	20.1875	118	100.4375	357.375	329.6875
DK	HC6	56.9375	68.4375	96	101.0625	51.3125	55.125	22.1875	22.5625	104	115.9375	330.4375	363.125
SK	HC7	15.9375	105.5	49.25	157.1875	23.9375	59.9375	11.125	31.375	24.8125	136.375	125.0625	490.375
SJ	HC8	70.5625	48.5	109.1875	115.5	41.625	41.75	23.25	18.8125	112.4375	88.8125	357.0625	313.375
VL	HC9	47.75	95.8125	103.125	134.8125	51.1875	57.875	20.25	30	78.4375	140.5625	300.75	459.0625
GK	HC10	64.625	85.625	76.875	137.375	30.375	40.375	14.4375	35.75	73.5	150.5	259.8125	449.625
HF	HC11	51.625	81.3125	97.25	150.3125	48.375	66.125	19.5	31.6875	128.375	169.0625	396.125	498.5
HK	HC12	53.8125	67.1875	96.3125	94.625	41.725	53.9375	18.625	19	82.375	90.5	316.375	325.25
YO	HC13	60.1875	76.5625	106.3125	124.0625	38.625	63.875	16.0625	38.4375	89.0625	117.75	358.25	385.1875
SG	HC14	62.75	94.8125	110.0625	144.5625	40.875	68.5	18.0625	34.4375	97.0625	140.0625	361.8125	482.375
Total		793.75	1180.25	1434	1894.563	597.725	786.1875	260.1875	385.6125	1389.313	1834.313	4630.5	6045.425

Corpus Callosum Volumetry

Statistical analysis of corpus callosum volume revealed significant differences between the OBPP cohort and healthy controls (see Table 4). The mean corpus callosum volume was lower in all segments of corpus callosum in OBPP cohort as compared to that in healthy controls.

Independent t-test revealed statistically significant volume loss in segments I, II, and IV, and narrowly missed significance mark in segment III (corresponding to fibers from primary motor region; see Figure 3/Table 5).

Resting-State fMRI Results

Test Hemisphere (Left) vs Internal Control (Right)

There is decreased activation in the sensorimotor network on the left (test) hemisphere, and is predominantly in the postcentral region. In the right hemisphere (internal control) of the patient, a total of 1401 voxels were activated in the sensorimotor network, compared to 715 voxels on the left side (test side; see Figures 4A and 4B/Table 1).

Test Hemisphere (Left) vs Corresponding (Left) Healthy Control

There is marked reduction in activation of sensorimotor network and extent of sensorimotor network in the test hemisphere as compared to the same side in healthy controls. A nonquantitative visual assessment reveals a shrunken and weakly activated sensorimotor network in test cohort. The activated number of voxels is more than thrice as large (3082 vs 715) in healthy subjects (see Figures 4B and 4D/Table 1).

Internal Control (Right) vs Corresponding (Right) Healthy Control

Although the activation is stronger on the internal control as compared to test side, it is still weaker than that in a healthy control, essentially amounting to only 60% of the healthy value (see Figures 4A and 4C/Table 1).

DISCUSSION

To the best of our knowledge, this is the first of its kind to study corpus callosum volumetry and application of rsfMRI of sensorimotor network in OBPP. It attempts to highlight the central effects of a peripheral, indirect, insult to the brain.

Cortical Plasticity and Application of rsfMRI

The sensorimotor network has been the point of interest in various studies on BPI,[34] and following peripheral nerve surgeries. Substantial literature exists which have demonstrated good correlation between the results of task-based fMRI and rsfMRI.[17,18,35–37]

An important difference between adult plasticity and developmental plasticity (which occurs in the developing brain) is that pediatric brain has a stronger plastic potential. Various growth factors are lost at various stages in the developmental period,[38] rendering plasticity more uncertain at later years.

Completion of peripheral innervation and physical integrity of the neural circuit is not equivalent to functional outcomes, although this is a mandatory first step. Unless "meaningful" cortical re-organization occurs, the "wiring" cannot be activated. This explains why some patients do well and some do not, despite a successful neurotization.[39] Sokki et al[20] demonstrated

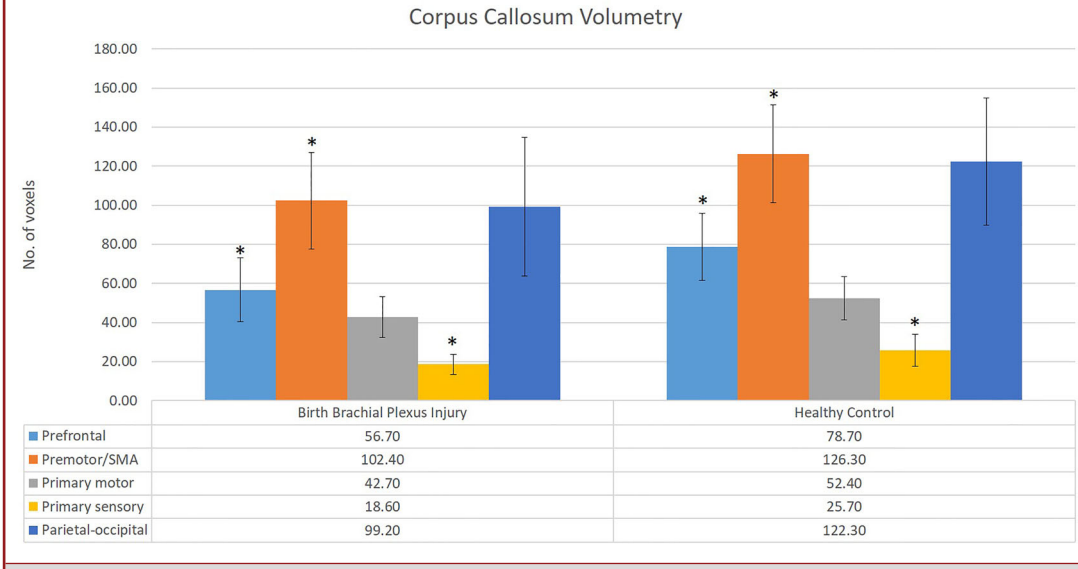

FIGURE 3. *Segmental corpus callosum volume in OBPP and healthy controls, with bars showing standard deviation. Segmentation is in accordance with the Hofer and Frahm[23] parcellation technique. Asterisk (*) indicates statistically significant differences in segmental volumes at P < .05.*

TABLE 5. Mean Corpus Callosum Volume in BPI and Healthy Controls

Corpus callosum segment	OBPP	Healthy control	*P*-value
Prefrontal	56.7 ± 16.49	78.7 ± 17.23	.019
Premotor/SMA	102.4 ± 24.71	126.3 ± 25.13	.046
Primary motor	42.7 ± 10.41	52.4 ± 10.96	.058
Primary sensory	18.6 ± 5.12	25.7 ± 8.21	.032
Parietal-occipital	99.2 ± 35.39	122.3 ± 32.47	.146

Results of t-test.

the importance of neural plasticity in adults following successful brachial plexus neurotization. Aberrant neuroplasticity is also responsible for phantom limb pain and post-brachial plexus avulsion neuropathic pain.[39,40] In fact, cortical plasticity helps in isolating respiration-synkinetic movements of the neurotized limb after an intercostal-musculocutaneous nerve transfer. With continued training, the subjects are able to isolate chest movements and limb movements.[20] In another work by our group (as yet unpublished), we have discussed the role of aberrant cortical reorganization in the pathogenesis of post-brachial plexus avulsion neuropathic pain, and how DREZotomy causes the expanded neighboring sensory territory in the brain to recede, thus alleviating the pain perception. Topographical changes have been found to occur following injury per se and following recovery—spontaneous or postsurgical. After a successful intercostal-musculocutaneous neurotization, there is initially a respiration-synkinetic movement, but with continued training, these patients were able to isolate these movements—an effect which is attributed to neuroplasticity.[20]

Our results highlight the lacunae we have in understanding the cortical plasticity and outcomes in OBPP. Although the reduction in activation of sensorimotor network on the side contralateral to injured limb is expected, we have also found decreased activation and shrunken area of activation in the internal control, as compared to that in healthy controls. It is a common understanding that the right and left hemispheres are inherently different in normal individuals.[41] Lateralization has been suggested to exist for visual, default mode, salience, and language networks in rsfMRI,[42,43] but it is unclear that there is differential activation of sensorimotor network on both sides. Newborns are believed to be ambidextrous, or probably with vacillating hand preference, and handedness is not clearly established at least until 1 yr of age.[44-46] We are not able to determine the equipotentiality of the hemispheres; thus, the assumption of internal control should be understood with this liability.

Corpus Callosum Volume Loss in OBPP

This study showed corpus callosum volume loss in subjects with OBPP. We suggest that this may be due to retrograde transneuronal degeneration. Chimelli et al[47] had performed sciatic nerve section in new-born rats. They demonstrated reduced number of both myelinated and unmyelinated axons in the ipsilateral corticospinal tract fibers in the spinal cord, and also decreased number of horseradish peroxidase-labeled cells in the contralateral sensorimotor cortex. This was the first description

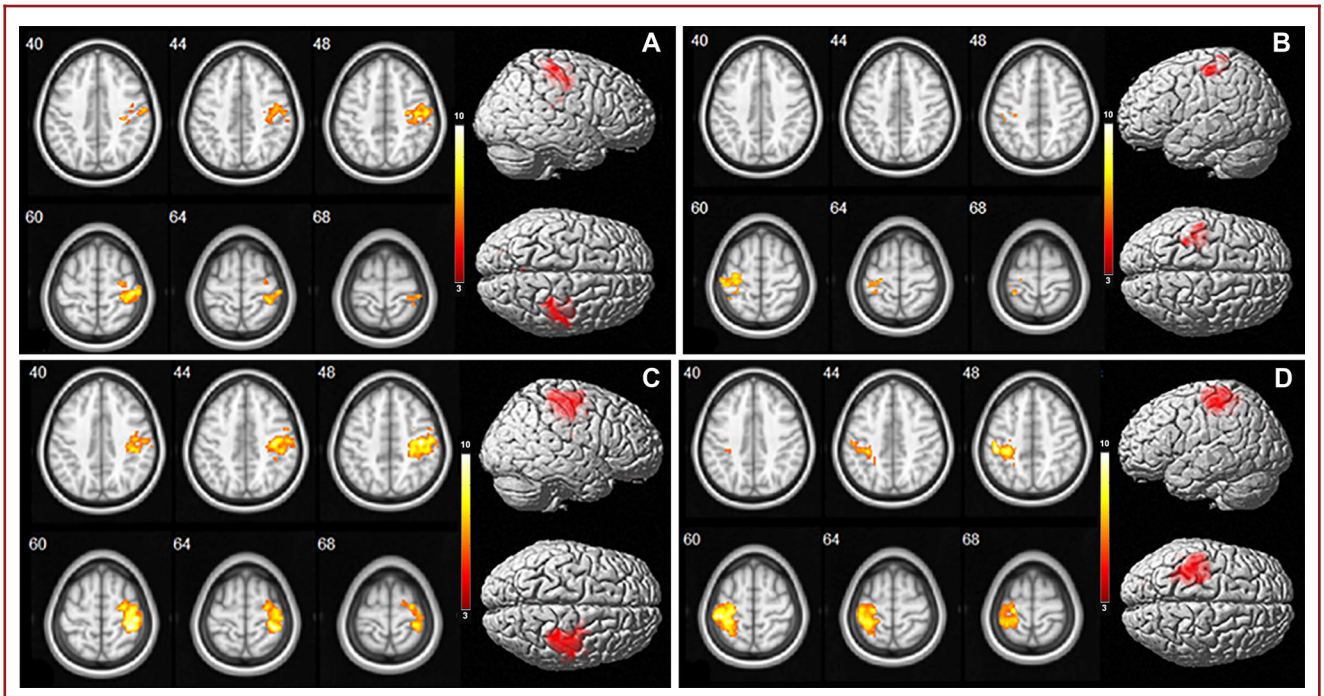

FIGURE 4. *Multislice and volume rendered view of sensorimotor network of ICA. In SPM format, on multislice axial view, anatomical right is on the right side of page and vice versa.* ***A****, Patient_right (internal control).* ***B****, Patient_left (test).* ***C****, Healthy Control_right.* ***D****, Healthy Control_left.*

of secondary transneuronal degeneration in the brain following a peripheral nerve injury. Since that study was also performed in new-born rats, it is comparable to OBBP.

In this study, significant loss of corpus callosum volume occurred in segments I, II, and IV, which correspond to fibers from prefrontal, premotor/supplementary motor, and primary sensory areas, respectively. This correlates well with the clinical picture. In the absence of sensorimotor inputs from the injured brachial plexus, there is consequent degeneration of fibers from the motor association areas, which are responsible for motor task planning and execution. Surprisingly, the volume loss in segment III (primary motor area) is not significant. It is possible that attempts at cortical plasticity in the primary motor area result in restoration of some volume. Diffusion tensor imaging (DTI) and white matter tractography[15,48] would probably give better answers regarding the functional integrity/repair of the white matter. We are looking into this aspect as well.

Corroborative Evidence for Role of Corpus Callosum in Interhemispheric Coactivation

An interesting observation is the decreased activity in the other half of the brain as well, in comparison with healthy controls. The detection of corpus callosum atrophy in this context points to its possible causative association with disruption of interhemispheric coactivation. Although some investigators have shown that corpus callosum is less important for sensorimotor interhemispheric connections, it may still be a possible contributing factor.[9,10,49] Further studies are needed to improve our understanding. In this regard, it may be worth studying other resting-state networks of the brain as well.

Limitations

Although the corpus callosum is a good marker for white matter volumetry, DTI and white matter tractography would give more insights into the integrity of white matter.

Also, in view of the findings suggestive of a global insult to the developing brain, a functional connectivity MRI would further enrich our understanding. We are studying this aspect and hope to contribute to further our understanding of pediatric brain.

CONCLUSION

This study has helped to gain new insights on the developing brain's response to insults. Corpus callosum atrophy in OBPP suggests existence of more profound central effects of a peripheral nerve injury on the brain than commonly thought. What may seem to be a peripheral nerve injury may well be translated into higher cortical as well as subcortical consequences like corpus callosum volume loss and subsequent disruption of bilateral connectivity in the brain. It needs to be further established whether this is a function of the location of the injury—peripheral—or timing of the injury—neonatal immature brain—or both.

Disclosures

This study is based on the thesis of Dr Kishore Kislay and part of the research was funded by Indian Council of Medical Research (ICMR) Thesis grant (3/2/Nov-2014/PG-Thesis-HRD-17). The authors have no personal, financial, or institutional interest in any of the drugs, materials, or devices described in this article.

REFERENCES

1. Dobbing J, Sands J. Quantitative growth and development of human brain. *Arch Dis Child* 1973;48(10):757-767.
2. Brody BA, Kinney HC, Kloman AS, Gilles FH. Sequence of central nervous system myelination in human infancy. I. An autopsy study of myelination. *J Neuropathol Exp Neurol* 1987;46(3):283-301.
3. Dietrich R, Bradley W, Zaragoza E, et al. MR evaluation of early myelination patterns in normal and developmentally delayed infants. *Am J Roentgenol* 1988;150(4):889-896.
4. Cowan WM. Anterograde and retrograde transneuronal degeneration in the central and peripheral nervous system. In: Nauta WJH, Ebbesson SOE, eds. *Contemporary Research Methods in Neuroanatomy*. Springer: Berlin Heidelberg; 1970:217-251. Available at: http://link.springer.com/chapter/10.1007/978-3-642-85986-1_11. Accessed November 17, 2016.
5. Beatty R, Sadun A, Smith L, Vonsattel J, Richardson E. Direct demonstration of transsynaptic degeneration in the human visual system: a comparison of retrograde and anterograde changes. *J Neurol Neurosurg Psychiatry* 1982;45(2):143-146.
6. Bridge H, Plant GT. Conclusive evidence for human transneuronal retrograde degeneration in the visual system *J Clin Exp Ophthalmol* 2012;S3:003.
7. Benavidez DA, Fletcher JM, Hannay HJ, et al. Corpus callosum damage and interhemispheric transfer of information following closed head injury in children. *Cortex* 1999;35(3):315-336.
8. Lou L, Shou T, Li Z, Li W, Gu Y. Transhemispheric functional reorganization of the motor cortex induced by the peripheral contralateral nerve transfer to the injured arm. *Neuroscience* 2006;138(4):1225-1231.
9. Johnston JM, Vaishnavi SN, Smyth MD, et al. Loss of resting interhemispheric functional connectivity after complete section of the corpus callosum *J Neurosci* 2008;28(25):6453-6458.
10. Hua X, Li Z, Xu W, Zheng M, Xu J, Gu Y. Interhemispheric functional reorganization after cross nerve transfer: via cortical or subcortical connectivity? *Brain Res* 2012;1471:93-101.
11. Ewing-Cobbs L, Prasad MR, Hasan KM. Developmental plasticity and reorganization of function following early diffuse brain injury. In: Nelson CA, Luciana M, eds. *Handbook of Developmental Cognitive Neuroscience*. London, UK: MIT Press; 2008:399-413.
12. Levin HS, Benavidez DA, Verger-Maestre K, et al. Reduction of corpus callosum growth after severe traumatic brain injury in children. *Neurology* 2000;54(3):647-647.
13. Bigler ED. Quantitative magnetic resonance imaging in traumatic brain injury. *J Head Trauma Rehabil* 2001;16(2):117-134.
14. Beauchamp MH, Anderson VA, Catroppa C, et al. Implications of reduced callosal area for social skills after severe traumatic brain injury in children. *J Neurotrauma* 2009;26(10):1645-1654.
15. Wu TC, Wilde EA, Bigler ED. Longitudinal changes in the corpus callosum following pediatric traumatic brain injury. *Dev Neurosci* 2010;32(5–6):361-373.
16. Rosazza C, Minati L. Resting-state brain networks: literature review and clinical applications. *Neurol Sci* 2011;32(5):773-785.
17. Lee MH, Smyser CD, Shimony JS. Resting-state fMRI: a review of methods and clinical applications *Am J Neuroradiol* 2013;34(10):1866-1872.
18. Lang S, Duncan N, Northoff G. Resting-state functional magnetic resonance imaging. *Neurosurgery* 2014;74(5):453-464; discussion 464-465.
19. Navarro X, Viv? M, Valero-Cabr? A. Neural plasticity after peripheral nerve injury and regeneration. *Prog Neurobiol* 2007;82(4):163-201.
20. Sokki AM, Bhat DI, Indira Devi B. Cortical reorganization following neurotization. *Neurosurgery* 2012;70(5):1305-1311; discussion 1311.
21. Dimou S, Biggs M, Tonkin M, Hickie IB, Lagopoulos J. Motor cortex neuroplasticity following brachial plexus transfer. *Front Hum Neurosci* 2013;7:500.
22. Mohanty CB, Bhat D, Indira Devi B. Role of central plasticity in the outcome of peripheral nerve regeneration. *Neurosurgery* 2015;77(3):418-423.
23. Hofer S, Frahm J. Topography of the human corpus callosum revisited—comprehensive fiber tractography using diffusion tensor magnetic resonance imaging. *NeuroImage* 2006;32(3):989-994.
24. Herron TJ, Kang X, Woods DL. Automated measurement of the human corpus callosum using MRI. *Front Neuroinform* 2012;6:25.
25. Adamson C, Beare R, Walterfang M, Seal M. Software pipeline for midsagittal corpus callosum thickness profile processing. *Neuroinformatics* 2014;12(4):595-614.
26. Smith SM, Jenkinson M, Woolrich MW, et al. Advances in functional and structural MR image analysis and implementation as FSL *NeuroImage* 2004;23(suppl 1):S208-S219.
27. Jenkinson M, Bannister P, Brady M, Smith S. Improved optimization for the robust and accurate linear registration and motion correction of brain images. *NeuroImage* 2002;17(2):825-841.
28. Smith SM. Fast robust automated brain extraction. *Hum Brain Mapp* 2002;17(3):143-155.
29. Beckmann CF, Smith SM. Tensorial extensions of independent component analysis for multisubject FMRI analysis. *NeuroImage* 2005;25(1):294-311.
30. Beckmann CF, Deluca M, Devlin JT, Smith SM. Investigations into resting-state connectivity using independent component analysis. *Philos Trans Roy Soc B: Biol Sci* 2005;360(1457):1001-1013.
31. Klein A, Andersson J, Ardekani BA, et al. Evaluation of 14 nonlinear deformation algorithms applied to human brain MRI registration. *NeuroImage* 2009;46(3):786-802.
32. Beckmann CF, Mackay, CE, Filippini N, Smith, SM. Group comparison of resting-state FMRI data using multi-subject ICA and dual regression. *NeuroImage* 2009;47:S148.
33. Filippini N, Macintosh BJ, Hough MG, et al. Distinct patterns of brain activity in young carriers of the APOE- 4 allele. *Proc Natl Acad Sci USA* 2009;106(17):7209-7214.
34. Qiu T-M, Chen L, Mao Y, et al. Sensorimotor cortical changes assessed with resting-state fMRI following total brachial plexus root avulsion. *J Neurol Neurosurg Psychiatry* 2014;85(1):99-105.
35. Zhang D, Johnston JM, Fox MD Preoperative sensorimotor mapping in brain tumor patients using spontaneous fluctuations in neuronal activity imaged with functional magnetic resonance imaging: initial experience. *Neurosurgery* 2009;65(6 suppl):226-236.
36. Kannurpatti SS, Rypma B, Biswal BB. Prediction of task-related BOLD fMRI with amplitude signatures of resting-state fMRI. *Front Syst Neurosci* 2012;6:7.
37. Rosazza C, Aquino D, D'Incerti L, et al. Preoperative mapping of the sensorimotor cortex: comparative assessment of task-based and resting-state fMRI. *PLoS ONE* 2014;9(6):e98860.
38. Eysel UT. Adult cortical plasticity. In: Squire LR, ed. *Encyclopedia of Neuroscience*. Oxford: Academic Press; 2009:141-147. Available at: http://www.sciencedirect.com/science/article/pii/B9780080450469002011. Accessed May 14, 2015.
39. Simon NG, Franz CK, Gupta N, Alden T, Kliot M. Central adaptation following brachial plexus injury *World Neurosurg* 2016;85:325-332.
40. Lotze M, Grodd W, Birbaumer N, Erb M, Huse E, Flor H. Does use of a myoelectric prosthesis prevent cortical reorganization and phantom limb pain? *Nat Neurosci* 1999;2(6):501-502.
41. Feng J, Liu H, Xu J, Gu Y, Shen Y. Differences in brain adaptive functional reorganization in right and left total brachial plexus injury patients. *World Neurosurg* 2015;84(3):702-708.
42. Liu H, Stufflebeam SM, Sepulcre J, Hedden T, Buckner RL. Evidence from intrinsic activity that asymmetry of the human brain is controlled by multiple factors. *Proc Natl Acad Sci USA* 2009;106(48):20499-20503.
43. Nielsen JA, Zielinski BA, Ferguson MA, Lainhart JE, Anderson JS, He Y. An evaluation of the left-brain vs. right-brain hypothesis with resting state functional connectivity magnetic resonance imaging. *PLoS ONE* 2013;8(8):e71275.
44. Gesell A, Ames LB. The development of handedness *J Genet Psychol* 1947;70(2):155-175.
45. Bates E, O'connell B, Vaid J, Sledge P, Oakes L. Language and hand preference in early development. *Dev Neuropsychol* 1986;2(1):1-15.
46. Nespoulous JL, Perron P, Lecours AR. *The Biological Foundations of Gesture: Motor and Semiotic Aspects*. Hove (UK): Psychology Press, 2014.

47. Chimelli L, Scaravilli F. Secondary transenuronal degeneration: cortical changes induced by peripheral nerve section in neonatal rats. *Neurosci Lett* 1985;57(1):57-63.
48. Bendlin BB, Ries ML, Lazar M, et al. Longitudinal changes in patients with traumatic brain injury assessed with diffusion-tensor and volumetric imaging. *NeuroImage* 2008;42(2):503-514.
49. Pawela CP, Biswal BB, Hudetz AG, et al. Interhemispheric neuroplasticity following limb deafferentation detected by resting-state functional connectivity magnetic resonance imaging (fcMRI) and functional magnetic resonance imaging (fMRI). *NeuroImage* 2010;49(3):2467-2478.

COMMENT

The effects of neonatal brachial plexus injury (NBPP) on the developing brain are still largely unknown. This very interesting paper uses fMRI to describe the effects of NBPP on corpus callosum volumetry, especially in the motor association areas. Unfortunately, due to the small number of patients and healthy controls that were included in the study, it was not possible to determine any statistical differences between operated and non-operated individuals. Nevertheless, this paper gives some minimal clues for explanation of several facts that are observed after a NBPP surgical reconstruction: patients showing adequate reinnervation of muscles that are not functionally used, bilateral activation of the cortex when performing a single-limb task, changes in language dominancy from the affected to the healthy hemisphere, or patients under 15 years old having a contralateral C7 transfer achieving independent control of both upper limbs. Future studies with a bigger number of patients will be more than welcomed in the future in order to further clarify these items and many others.

Mariano Socolovsky
Buenos Aires, Argentina